Elastic and Thermal Properties of SiO_2 Glass

Hiroshi KOBAYASHI[1], Toshio KOSUGI[2], Yoshiaki KOGURE[3]

[1] National Research Laboratory of Metrology, Tsukuba, Ibaraki 305, Japan

[2] Faculty of Science, Hiroshima University, Naka-ku, Hiroshima 730, Japan

[3] The Nishi Tokyo University, Kitatsuru-gun, Yamanashi 409-01, Japan

Abstract: Some elastic and thermal properties of SiO_2 glass are described.1)Load-elongaton curves of SiO_2 fibers a few μm in diameter were measured, and they showed nonlinearity and a distinct elastic hysteresis. 2)Raman spectra were obtained for SiO_2 fibers of 125 μm diameter at tensile strains ranging from 0 to 3.5 %. The spectrum for the main peak at 440 cm^{-1} decreased in height with an increase in the tensile strain. 3)The thermal expansion of SiO_2 fibers synthesized by the sol-gel method was measured in the temperature range of 100 to 300 ℃. Fibers as grown represented shrinkage of length, but after enough annealing they represented low thermal expansion. 4)Internal friction of SiO_2 glass with excessive Oxygen ($10^{17}/cm^3$) was measured in the temperature range of 4.2 K to room temperature. The doping of oxygen to SiO_2 glass showed a slight increment of internal friction at the same temperature as pure SiO_2

glass. 5)Internal friction of SiO_2 glass was measured in temperature ranging from 4.2 K to room temperature and pressure ranging from 0.1 M to 1 GPa. With an increase in the pressure, Internal friction shifts its peak temperature to the higher sides.

1) Anharmonicity and Elastic Hysteresis of Fused SiO_2 Fibers[1]

The fact that the load-elongation relation of a fused SiO_2 fiber shows nonlinearity was first reported by Hillig[2]. Mallinder et al.[3] and Powell et al.[4] also observed the deviation of load-elongation curves from straight lines in fused SiO_2 fibers and soda-glass fibers. However, the load-elongation curves for these fibers differed in the nature of the deviation from linearity. The fused SiO_2 fibers showed an increase in Young's modulus with increasing strain, whereas the soda-glass fibers showed a corresponding decrease in Young's modulus. Hyodo et al.[5] found the same type of nonlinear curves and, in addition, an elastic hysteresis in soda-glass fibers. Moreover, they also found that the load-elongation curves of fused SiO_2 fibers show a trace of mechanical loss at low temperature, although the loss was too small to be measured.

Similar nonlinear curves have been observed both in copper[4,6] and silver whiskers,[4,7] but these curves show no distinct hysteresis. The nonlinearity observed in the load-elongation curves of metal whiskers is explained in the following way; in crystals, interatomic forces are nonlinear with respect to atomic displacements and this nonlinearity appears as thermal expansion, as is well known. The load-elongation curves of metal whiskers observed were in good agreement

with those calculated by higher-order elastic theory,[8-10] which treats anharmonic properties of solids.

The tensile-testing machine for fiber specimens which was prepared by the authers[7] is composed of an analytical balance and an electro-optical lever which is similar to that by Jones et al.[11] The reading capability of this machine is 0.05 μm in length and 1 mg in load. Pure SiO_2 fibers were tested in room temperature. Fibers a few μm in diameter were obtained by blowing in the flame fibers 200-300 μm in diameter. The specimens suitable to be tested were selected from the lot of fibers like wool under a microscope. Specimens selected in this way were straight and clean in the surface. The diameter of fibers was measured on the glass plate by a microscope with a scale and the length of them glued to the experimental apparatus by a telescope with a scale. The adhesives used were diphenylcarbazide cement and aron-alpha(α-cyanoacrylate).

The relation between stress P and strain ε of a fused SiO_2 fibers is shown in Fig. 1, which exhibits a distinct nonlinear load-elongation curve and an elastic hysteresis. The dashed line is the Hookian approximation based on the experimentally determined zero-stress Young's modulus. The apparent nonlinearity in the neighborhood of the origin is assumed to be caused by the misalignment of the specimen with respect to the stress axis. The load and the elongation at the points which are determined as the cross points of the coordinates and the dashed line are about 40 mg and 1 μm. The relation

between strain/stress : ε /P and stress P is shown in Fig. 2 to confirm that strain ε is expressed as a second-order function of stress P as is described in Ref. 7. Observed curves of fibers show reproducible traces; when the applied force is stopped during the second test and force is released, the second curve takes the same trace as that obtained in the first test, except for a small deviation at the top of the curve. According to higher-order elastic theory, the nonlinear relation between stress P and strain ε ($P=F/S_0$; F is the applied force to a specimen and S_0 is the cross sectional area before deformation) is expressed as follows[4,12];

$$\varepsilon = (P/E) + \delta (P/E)^2 \tag{1}$$

where E is Young's modulus and δ is the nonlinear constant which can be represented as a function of second- and third-order elastic constants. For a cubic crystal with the (100) axis, Young's modulus E, Poisson's ratio ν, and the nonlinear constant δ are given by

$$E = C_{11} - 2C_{12}\nu \tag{2}$$

$$\nu = C_{12}(C_{11}+C_{12})^{-1} \tag{3}$$

$$\delta = -3/2 + [C_{11}(C_{11}+C_{12}) - 2C_{12}^2]^{-1} \times \{1/2[2C_{12}\nu^2 - (C_{11}+C_{12})]C_{111}$$

$$+[(2C_{12}-C_{11})\nu^2+2C_{11}\nu+C_{12}]C_{112}$$

$$-[(C_{11}+C_{12})\nu^2+2C_{12}]C_{123}\}. \quad (4)$$

For an isotropic specimen, the number of independent elastic constants are reduced according to the relation $C_{44}=1/2(C_{11}-C_{12})$ for second-order elastic constants and $C_{112}=C_{123}+2C_{144}$, $C_{166}=C_{144}+2C_{456}$, and $C_{111}=C_{123}+6C_{144}+8C_{456}$ for third-order elastic constants. The experimental values of second- and third-order elastic constants of fused quartz have been reported by Bogardus[13]. Using these values for a fused SiO_2 fiber, Young's modulus E is 7.45×10^3 kgf/mm^2 (7.31×10^{11} dyn/cm^2), Poisson's ratio ν is 0.1684, and the nonlinear constant δ is -3.7. By fitting Eq. (1) to the increasing lines of the load-elongation curves using the least-squares method, experimental values were obtained and the results are shown in Table I . It is supposed that in this analysis, the intrinsic elastic deformation is reduced as much as the order of the hysteresis. The results show qualitative agreement between the calculated value of δ and the experimental ones, but the measured values are about an order of unity less than the calculated one. The experimental values of Young's modulus given by the present method are approximately 30 % less than the calculated one. The elastic hysteresis observed in the curves shown in Fig. 1 suggests the existence of some frictional processes in which deformation of the fiber recovers to the original state. Hyodo et al.[5] elongated soda-glass fibers in liquid nitrogen up to 13 % in strain, using an Instron-type tensile-testing machine and ob-

served the load-elongation curves also showing elastic hysteresis. They have explained the Hyodo-Togami model which takes into account the breaking and recovering of the pinning elements of SiO_2 network in the process.

In the present study, the nonlinear load-elongation curves have been observed in fused SiO_2 fibers and it is considered that the nonlinearity originates from the anharmonic interactions between atoms.[6] Moreover, a distinct elastic hysteresis in which the increasing curve takes a different trace from the decreasing one and then returns to the origin reproducibly has been found. According to Mozzi et al.[14] random network of fused SiO_2 is constructed of tetrahedrons in which each Si atom is surrounded by four oxygen atoms with a Si-O distance of about 1.62 A. Each oxygen atom is bonded to two Si atoms. The Si-O-Si bond with angle α shows a distribution of from 120° to 180° , with maximum at α =144° . The wide distribution of the Si-O-Si bond angle accounts for the possibility that SiO_2 fibers show soft mechanical properties constituting a random network. For a relaxation mechanism showing elastic hysteresis, it is supposed that when stress is applied to a specimen, tetrahedrons change their relative positions at the corners which are the sites of oxygen atoms, and when stress is released they return to their original configuration through some relaxation process. In order to study the relaxation mechanism of SiO_2 fibers, Raman spectroscopic study of SiO_2 fibers up to a few percent at room temperature was attempted.

2) Raman Spectra of SiO_2 Fibers at High Tensile Strain[15]

In the Raman spectrum of SiO_2 glass, there are a main, relatively broad, peak at 440 cm^{-1} and two lower but sharper peaks near 490 and 604 cm^{-1}. The latter two peaks are reduced by annealing and susceptible to neutron irradiation of SiO_2 glass[16]. In this study, by deconvoluting the raman peaks into Gaussian components, we suggest that the stress induced change at 440 cm^{-1} is caused by the distortion of the SiO_4 tetrahedron. The sample used were synthetic silica fibers of 125 μm diameter and coated with silicone-resin. They were fabricated by the VAD (vapor-phase axial deposition) method. Fig. 3 shows an experimental set-up. A terminal portion of the fiber, where the silicone-resin was removed, was cemented to the calipers of a micrometer with an adhesive (Aron Alpha). The fiber was strained only between the calipers with a distance of 16.5 mm. A 514.5 nm argon ion laser beam with a 0.85 W output was focused to another end of the fiber. The scattered light emanating from the strained fiber portion was partly introduced into a double monochrometer and led to a photomultiplier. The light intensity, measured with a photon counter, was recorded as a function of wave number.

Fig. 4 shows the Raman spectra obtained from the SiO_2 glass at 0 % and 3.5 % tensile strain. The dominant peak at 440 cm^{-1} is seen to be lower at 3.5 % than at 0 % strain. Fig. 5 illustrates the results of a deconvolution of these spectra into Gaussian components: They are assigned to normal vibrational modes of SiO_4 or Si_2O. Hereafter we will principally discuss the change in the V4 mode spectrum due to

tensile stress in connection with the glass network structure.

We can presume that the stress-induced change in bond length must be negligible in comparison with that in bond angles in a stress range such as used in this study, since the force constants for bond-stretching are much greater than those for bond-bending. In other words, stress-induced change in Si-O-Si bond angle θ and O-Si-O bond angle ψ must play a significant role in the present analysis of Raman spectrum. In a previous study, however, no tensile stress effects were observed regarding Si-O-Si triangle modes[17]. This indicates that the average of θ is scarcely affected by tensile stress, though θ for each triangle in the glass network may increase or decrease depending on the direction of the Si-Si bond of the triangle concerned , e. g., on whether the direction is parallel or orthogonal to stress axis. On the other hand, the distortion of a SiO_4 tetrahedron shown in Fig. 6 must be induced by the uniaxial stress no matter what direction the tetrahedron has (i.e. a tetrahedron has no direction for the sake of symmetry). We defined the O-Si-O bond angle α and β in the manner shown in Fig. 6, and calculated the stress dependence of each normal mode frequency of the SiO_4 tetrahedron on α. The results are shown in Fig. 7, where the dashed line indicates the value at no stress (=109.5°). The tetrahedron has four normal mode, i.e. a non-degenerate V1 (808 cm^{-1}), a doubly degenerate V2 (250 cm^{-1}) and two triply degenerate V3 (1065 cm^{-1}), V4 (455 cm^{-1}) modes. One can see in Fig. 7 that two triply degenerate modes (V3 and V4) become clearly decoupled into a no-degenerate and a doubly degenerate mode with an increase in the deviation of α from 109.5° .

Hence, it seems very plausible that, as illustrated in Fig. 8, the tensile stress will cause shifts in the two decoupled modes and thus change the shape of the V4 mode component. Though the same change is expected for the V3 mode (1065 cm^{-1}) as that in the V4 mode, such change could not be observed in the present study, probably because of the very low intensity at 1065 cm^{-1} equivalent to that of background noise.

We conclude that, under 3.5 % strain, stress induced effects on the Raman spectra of SiO_2 glass network manifest themselves by way of the distortion of tetrahedrons, and not by way of the bond-to-bond elongation nor of the bond breaking.

3) Thermal Expansion of Sol-Gel SiO_2 Glass Fibers[18]

Thermal evolution of the sol-gel glass has attracted a great deal of interest in the fields of glass production and the development of glass with low thermal expansion. The types of thermodynamic behavior which occur during the conversion of gels to glasses have been reviewed thoroughly by Brinker et al.[19] and Scherer et al.[20]. They propose that: (1) capillary contraction, (2) condensation polymerization, (3) structural relaxation and (4) viscous sintering are the principal gel densification mechanisms. Any of these processes involves the shrinkage of volume with the increment of temperature. On the other hand, after adequate annealing, the glass represents low thermal expansion. In order to obtain a glass with low thermal expansion, TiO_2-SiO_2[21,22] and CuO-Al_2O_3-SiO_2[23] sol-gel glass have been synthesized and tested in regard to physical, chemical and thermal

properties. Thermal shrinkage and expansion of the glass have been investigated in different stages, but they are thought to be the properties of the same glass specimen. We measured the thermal expansion of the same glass fibers as grown and after annealing continuously, which represent the thermal expansion coefficients with a different sign.

The measuring system is essentially the same as that described by Imai and Bates[24], which consists of a laser interferometer to detect absolute displacement with the sensitivity of 10 nm and a clamping mechanism with a corner cube at each end of the specimen. A thermocouple was set at the center of the specimen without contact. Objects including the specimen were placed in a vacuum chamber inside a furnace. The SiO_2 glass fibers used were provided by the Asahi Glass Co., which were fabricated using a sol--gel process. Fibers 10 μm in each diameter were spun from sol under room temperature and bundled into 250 pieces, and then sintered in a furnace at 900 ℃. A sheaf of 250 pieces was clamped between two stages and the weight of 1 g was applied in order to keep the fibers straight. The length of the specimen was 50-100 mm

The thermal expansion of sol-gel SiO_2 glass fibers bundled into 250 pieces of 74.5 mm in length l_o was measured in the temperature range of 100 to 300 ℃. In Fig. 10, the displacements of the lengths of the fibers are shown from 100 to 300 ℃. The marks ○ indicate the displacement change before annealing, where the shrinkage in length is

recognized. On the other hand, marks + indicate that of the same fibers after annealing, where the linear expansion is recognized. Thermal expansion coefficients are calculated to be $1.6\text{-}2.4\times 10^{-7}$ $^{\circ}C^{-1}$. It should be noted that the annealing changes thermal expansion coefficients from negative values to positive ones. Negative thermal expansion, that is, the shrinkage of the fibers is supposed to exist because they remain in the sintering process and the positive one because they show the properties of true glasses. Sintering is the structural change of the glass and thermal expansion is the appearance of anharmonic interactions between atoms.

4) Internal Friction of SiO_2 Glass with Excessive Oxygen

It has been well known that SiO_2 glass shows a large and broad peak in internal friction at 30-35 K, which is about 100 times larger than a SiO_2 crystal. This peak is thought to be caused by the bending of the bridging oxygen atoms in the Si-O random network.[25] On the other hand, Awazu and kawazoe[26] reported that O_2 molecules which unexpectedly dissolve in the glasses strongly influence the optical properties. They proposed the reaction model to be O_2 (trapped) $\rightarrow$ 2 O ($\hbar\nu > 5.1$ eV) and O + O_2 $\rightarrow$ O_3 (trapped), in which the molecules behave as well as when they exist in the gas phase. It is very interesting how these molecules behave under applied stress. We measures the internal friction (ultra sonic attenuation at 51 kHz)[27] of a SiO_2 single crystal, pure SiO_2 glass and SiO_2 glass with excessive oxygen ($10^{17}/cm^3$) in the temperature range from 4.2 K to room temperature. Fig. 11 shows the internal friction Δ of a SiO_2 crys-

tal, in which the peak at 40 K is explained to be related with the impurities of Na ions. Fig. 12 shows the internal frictions Δ of a pure SiO_2 glass and the one with excessive oxygen, in which the solid and dashed lines indicate the frictions of the former and the latter respectively. We could not recognize any original peak related to the excessive oxygen. However, it is assumed that the doping of oxygen to SiO_2 glass shows a slight increment of the internal friction at the same temperature. The doped oxygen probably enhances the internal friction caused by the bridging oxygen atoms, that is, these oxygen atoms, which are thought to exist in the gas phase, increase the viscosities acting on the oxygen atoms in the random network.

5) Internal Friction of SiO_2 Glass under Low Temperatures and High Pressures

In most amorphous materials, the peaks of internal friction have been observed at temperatures of a few 10 K. These are the same as seen in the relaxation process, called Snoek peaks which originate from the point defects in crystals. Their frequencies (ω) depend on the equation $\omega\tau/[1+(\omega\tau)^2]$ and represent the maximum at the condition $\omega\tau=1$.

These phenomena observed in SiO_2 glasses are concerned with the transition of bridging oxygen atoms occupying the two stable sites. Since their oxygen atoms change the sites according to the thermal activation process, the relaxation time (τ) shows an Arrhenius type temperature dependence; $\tau \propto \exp(U/kT)$, where the activation energy U distributes and then the peak width is wide.

We measured the ultrasonic attenuation (12 MHz) of SiO_2 glass in the temperature range of 4.2 K to room temperature and in the pressure range of 0.1 M to 1 GPa. The SiO_2 glass used in this experiment was a columm 8 mm in diameter and 14 mm in length, and X-cut quartz crystal was used as a transducer. The high pressure apparatus is a piston-cylinder type one and the pressure vessel was placed in a He cryostat for the complete temperature and pressure ranges. The results are shown in Fig. 13. Under 0.1 MPa of pressure, the attenuation represents the broad peak at 35 K, but with an increase in pressure, it shifts the peak temperature to the higher sides. This is explained by the idea that the activation energy increases its value together with increasing pressure. In Fig. 14, the relation between the peak temperatures and the pressures is shown, and the activation volume which is determined from the relation is 7.2 A^3.

References

(1) Kobayashi H. J. Appl. Phys. 1987, 49, 4776.

(2) Hillig W. B. Modern Aspects of the Vitreous State, edited by MacKenzie J. P. (Butterworths, Lodon) 1962, vol.II , 189.

(3) Mallinder F. P.; Procter B. A. Phys. Chem. Glasses 1964, 5, 91.

(4) Powell B. E.; Skove M. J. Phys. Rev. 1968, 174, 977.

(5) Hyodo S.; Togami Y. J. Appl. Phys. 1973, 44, 2237.

(6) Kobayashi H.; Hiki Y. Phys. Rev. 1973, 7, 7.

(7) Kobayashi H.; Hiki Y. Jpn. J. Appl. Phys. 1972, 11, 737.

(8) Murnaghan F. C. Finite Defomation of an Elastic Solid, (Wiley, New York) 1951.

(9) Birch F. Phys. Rev. 1974, 71, 809.

(10) Thurston R. N.; Brugger K. Phys. Rev. 1964, A133, 1604.

(11) Jones R. V.; Richard J. C. S. J. Sci. Instrum. 1959, 36, 90.

(12) Seeger A.; Buck O. Z. Naturforsch. 1960, A15, 1056.

(13) Bogardus E. H. J. Appl. Phys. 1965, 36, 2504.

(14) Mozzi R. L.; Warren B. E. J. Appl. Crystallogr. 1969, 2, 164.

(15) Kobayashi H.; Ema K. The Physics and Technology of Amophous SiO_2, edited by Devine R. A. C. (Plenum Press, New York) 1988, 71.

(16) Stolen R. H.; Walrafen G. E. J. Chem. PHys. 1976, 64, 2623.

(17) Ema K.; Hibino Y.; Shigekawa H.; Hyodo S. Jpn. J. Appl. Phys. 1987, 26, 649.

(18) Kobayashi H.; Yamaguchi Y. to be published on Jpn. J. Appl. Phys. 1990, 29, L2089.

(19) Brinker C. J.; Scherer G. W.; Roth E. P. J. Non-Cryst. Solids

1985, 72, 345.

(20) Schere G. W.; Brinker C. J.; Roth E. P. J. Non-Cryst. Solids 1985, 72, 369.

(21) Hayashi T.; Yamada T.; Saito H. J. Mater. Sci. 1983, 18, 3137.

(22) Deng z.; Breval E.; Pantano C. G. J. Non-Cryst. Solids 1988, 100, 364.

(23) Tsuchiya T.; Yoshino S.; Fukuoka M.; MacKenzie J. D. J. Non-Cryst. Solids 1988, 100, 284.

(24) Imai H.; Bates W. J. Phys. E 1981, 14, 883.

(25) Anderson O. L.; Bommel H. E. J. Amer. Ceramic Soc. 1955, 38, 125.

(26) Awazu K.; Kawazoe H. J. Appl. Phys. 1990, 68, 3584.

(27) Schwarz R. B. Rev. Sci. Instrum. 1977, 48, 111.

Table I . Values of the nonlinear constant δ obtained by experiment.

Specimen	Length (cm)	Diameter (μm)	Nonlinear constant δ
1	1.26	4.4	−3.5
2	1.12	6.0	−2.0
3	0.97	4.1	−2.9

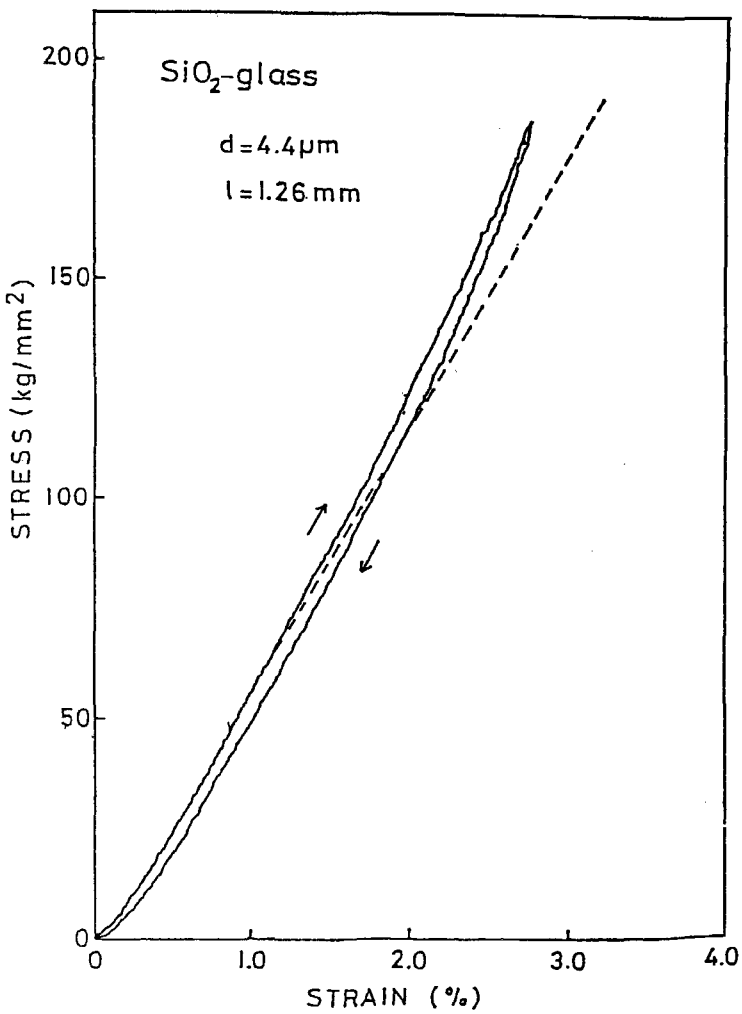

Fig.1. A nonlinear load-elongation curve of a fused SiO2 fiber 4.4 μm in diameter and 1.26 mm in length.

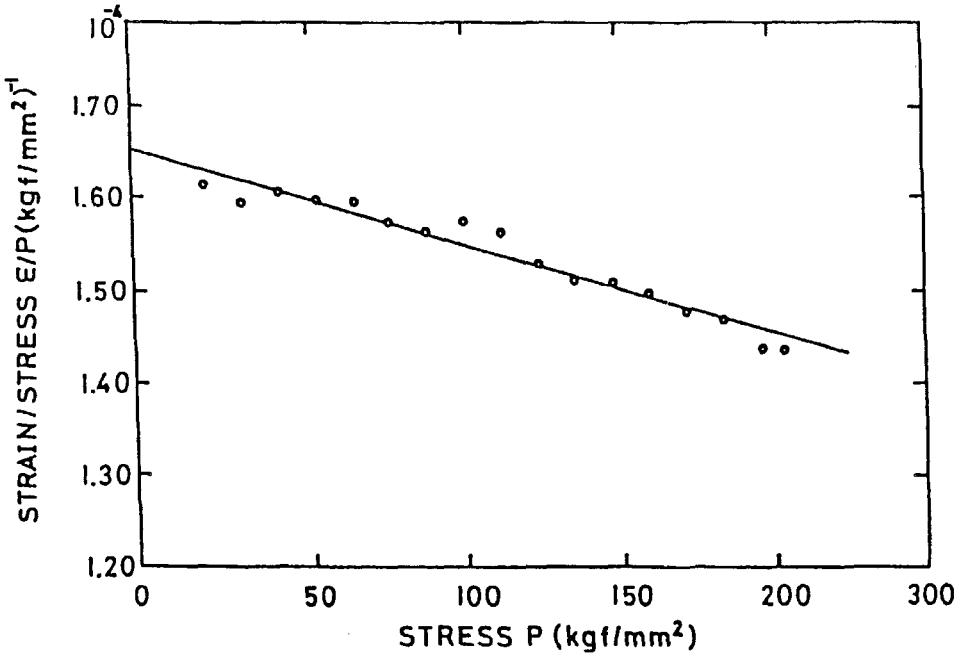

Fig.2. Relation between strain/stress ε /P and stress P.

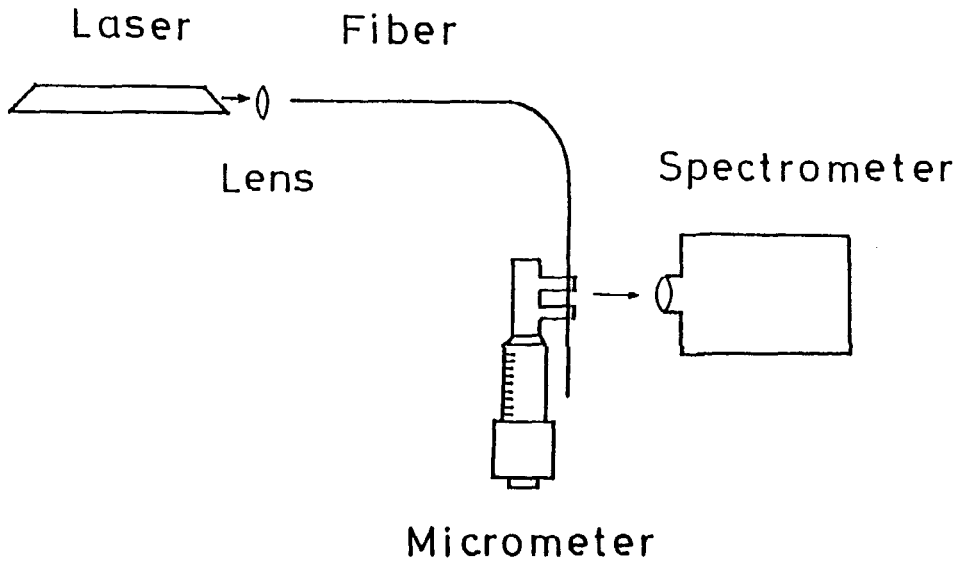

Fig.3. Experimental set-up for measuring Raman spectra.

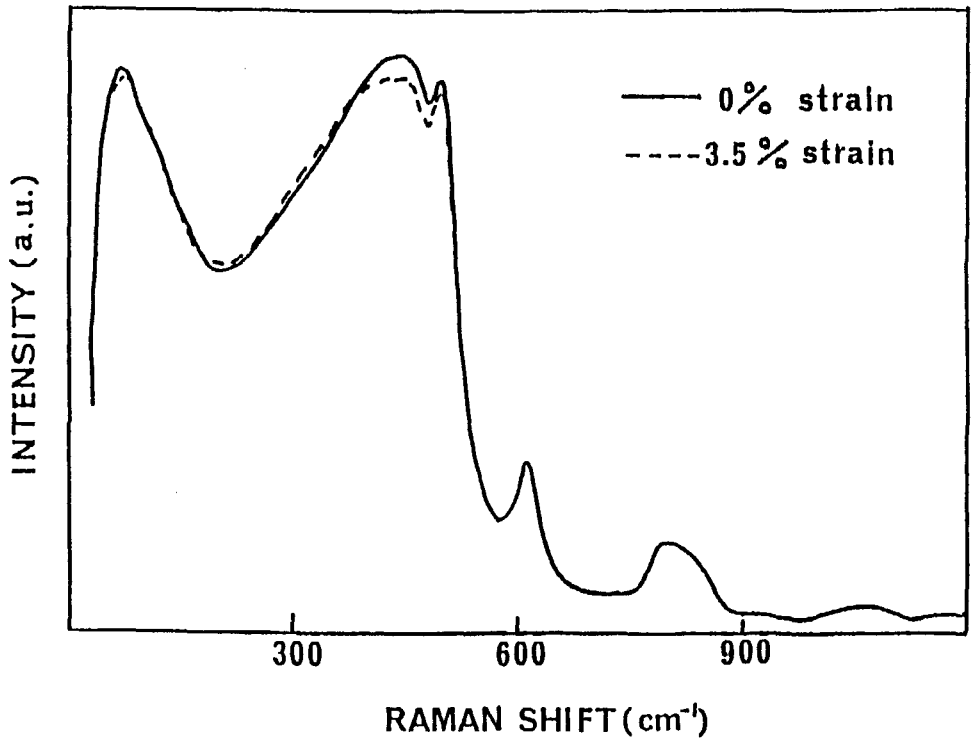

Fig.4. Raman spectra for a SiO_2 fiber at 0 and 3.5 % tensile strains.

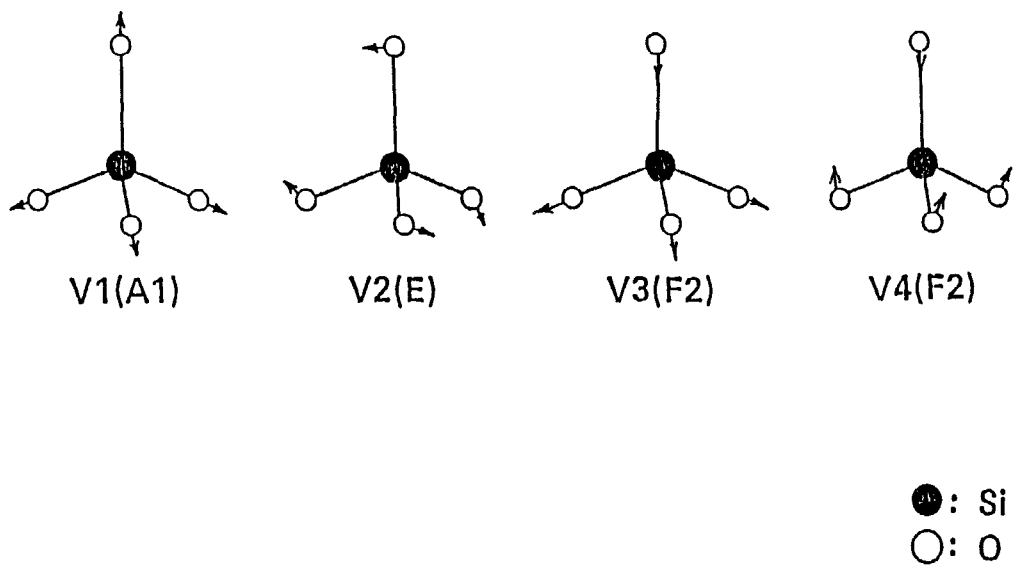

Fig.5. Normal vibration modes of a tetrahedral molecule SiO_4.

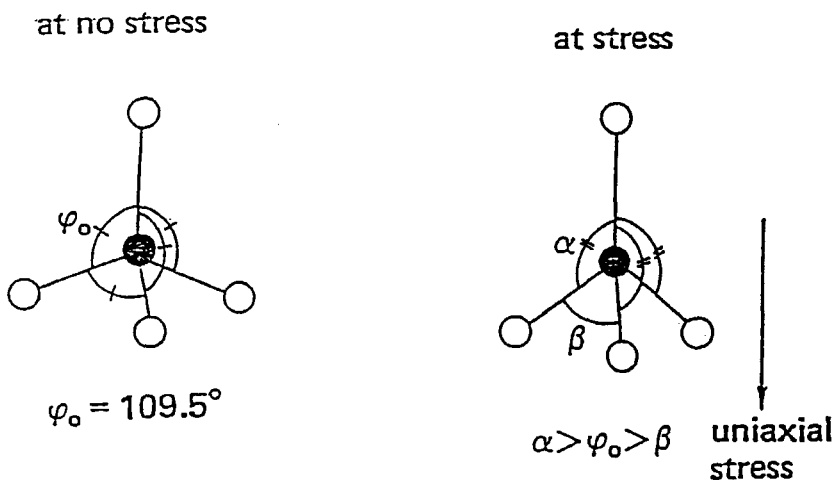

Fig.6. Schematic illustration for the distortion of a tetrahedral molecule SiO_4 under uniaxial stress.

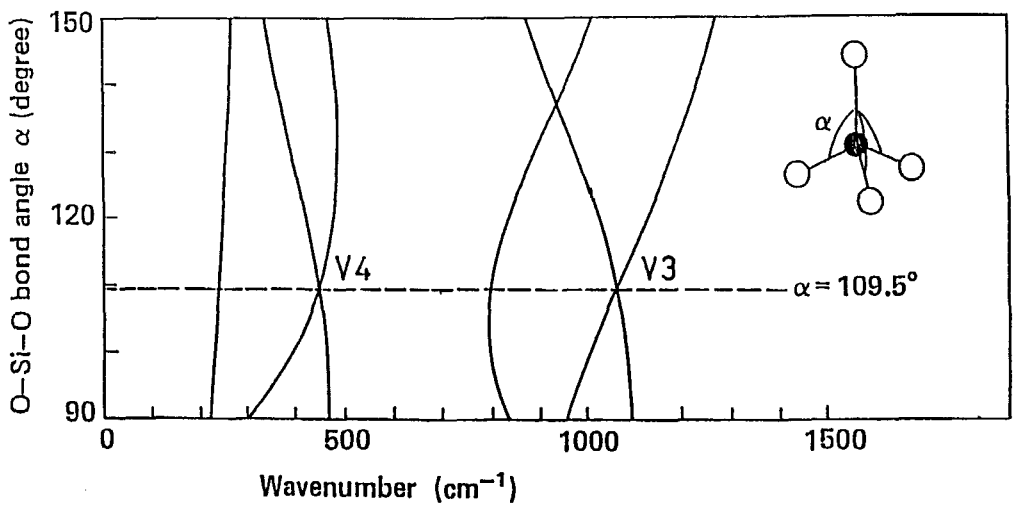

Fig.7. Wavenumber for normal mode vibrations of a SiO_4 tetrahedron as a function of α .

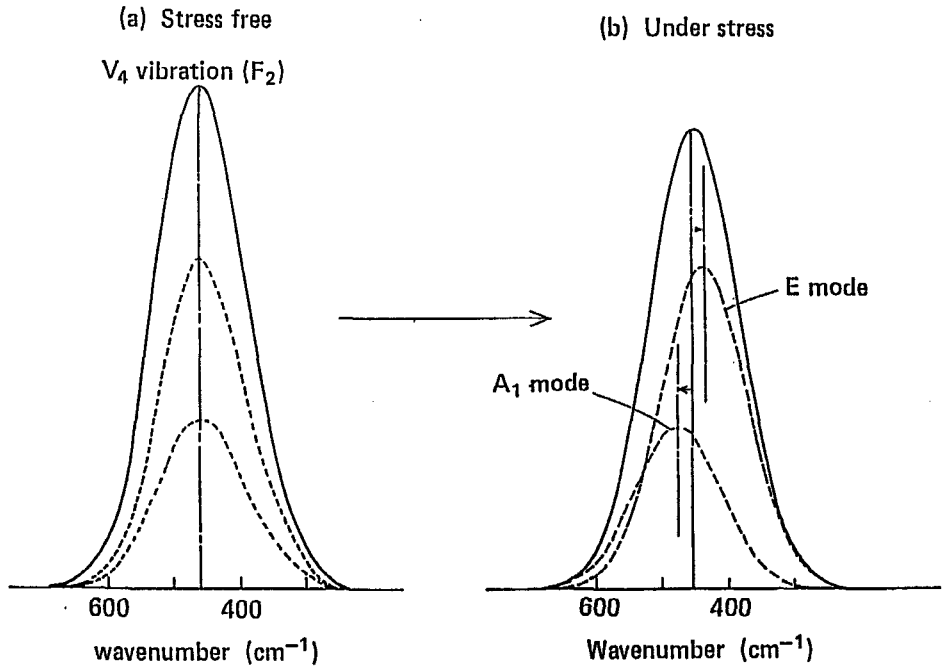

Fig.8. Reduced intensity change associated with the stress-caused decoupling of the V4 mode into a nondegenerate A1 and a doubly degenerate E modes.

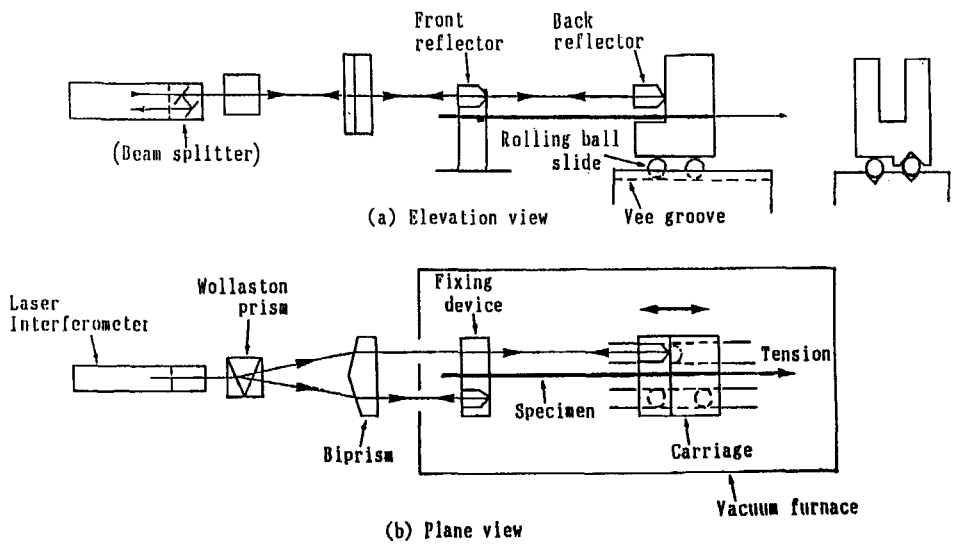

Fig.9. Experimental set-up for measuring thermal expansion.

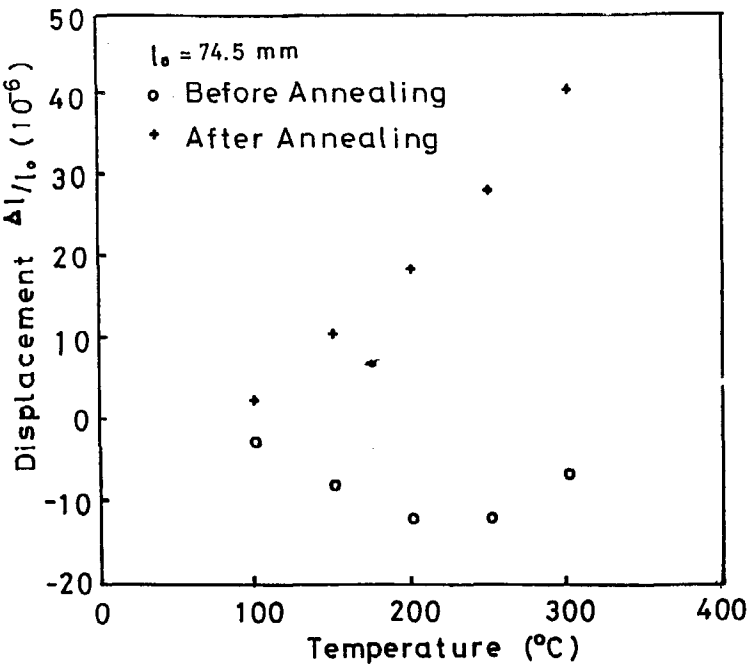

Fig.10. Displacements of the lengths of the sol-gel SiO_2 fibers from 100 to 300 °C.

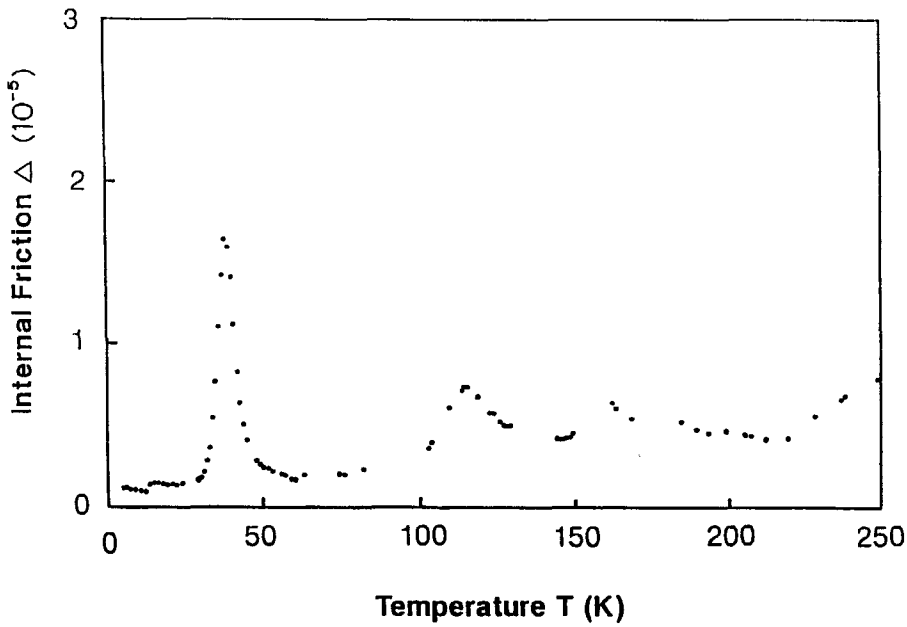

Fig.11. Internal friction △ of a SiO_2 crystal.

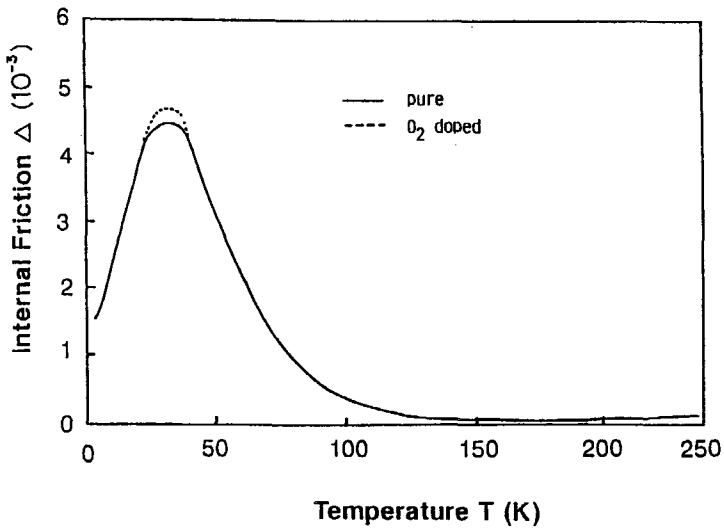

Fig.12. Internal friction △ of a pure SiO_2 glass and the one with the excessive oxygen ($10^{17}/cm^3$).

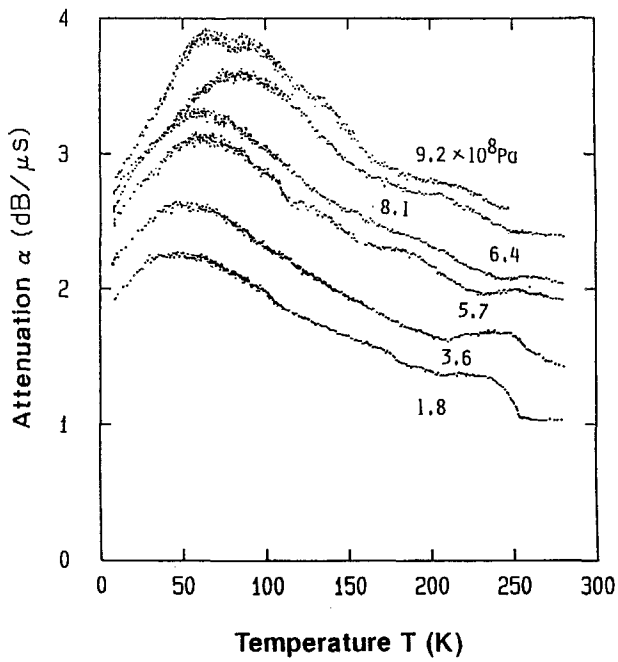

Fig.13. Ultrasonic attenuation α of a pure SiO_2 glass under high pressures.

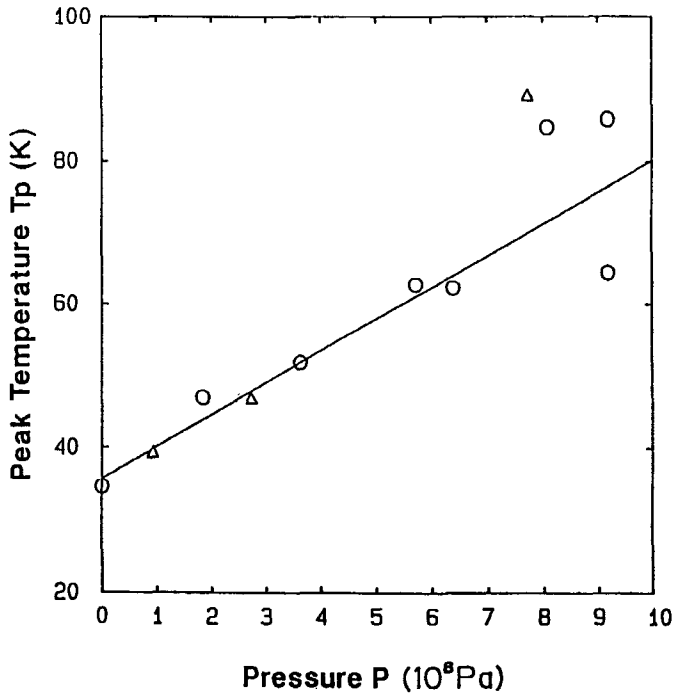

Fig.14. Pressure change of the peak temperatures Tp of ultrasonic attenuations.